

## Atom dynamics between conducting plates

S. Al-Awfi and M. Babiker

*Department of Physics, University of Essex, Colchester, Essex CO4 3SQ, England*

(Received 29 December 1997; revised manuscript received 10 April 1998)

The dynamics of atoms subject to laser light propagating between perfectly conducting parallel plates is investigated. In the semiclassical approximation the motion of atoms in this context is governed by a van der Waals-type potential, together with a dynamic dipole potential that comes into play as soon as a cavity mode is excited. In addition, the atoms become subject to an average dissipative (spontaneous) force associated with the cavity mode that always acts parallel to the plates. We show that, by a suitable choice of field intensity and detuning, the total transverse potential can be used to confine atoms in transverse vibrational states, while their motion in the parallel direction is controlled by the dissipative force. Significant variations of the characteristics of the system with atom velocity, dipole orientation, and type of excited cavity mode are emphasized. These features are illustrated using typical parameters for the case of sodium atoms between parallel plates with subwavelength separations. [S1050-2947(98)03709-3]

PACS number(s): 32.80.Pj, 32.80.Lg, 42.50.Vk

### I. INTRODUCTION

Recent research on the motion of atoms in spatially varying light fields has led to remarkable advances in atom cooling and trapping [1] and has culminated in the emergence of atom optics as a new field of research. The ultimate goal of atom optics is to achieve the routine generation of coherent atomic beams by means of atom lasers and be able to manipulate them using quantum atom optical elements such as beam splitters and atom mirrors [2]. Atom guides potentially form another important class of atom optical elements that is currently receiving considerable attention.

The operation of a typical atom guide makes use of spatially varying light fields either in free space [3] or confined within metallic or dielectric interfaces [2] and relies on the principle that appropriately detuned atoms are either attracted to or repelled from regions of high intensity. Recent work by Renn *et al.* [4] has demonstrated the action of atom guides that take the form of hollow cylindrical waveguides based on the configuration suggested earlier by Ol'Shanii, Ovchinnikov, and Letokhov [5]. In this kind of atom guide, to be referred to as the first kind, electromagnetic modes are set up in which field intensities are either maximum or minimum on the axis and so can be made to attract appropriately detuned atoms to the axial region as they are guided along the structure. The second kind of atom guide is based on evanescent fields at the guide walls [6–8] and the operation of this type of guide too was demonstrated by Renn *et al.* [9]. The evanescent fields at the dielectric walls of hollow cylindrical waveguides generate mirror action, repelling atoms away from the walls as they move along the axis. More recent experimental work on evanescent mode guiding of atoms through single-mode hollow optical fibers was done by Ito *et al.* [10].

In addition, planar waveguide structures have been considered. An evanescent mode parallel plate atom guide has been suggested by Dowling and Gea-Banacloche [2], while Sandoghdar *et al.* [11] have succeeded in controlling atomic motion within a gold two-plate microcavity of typical dimensions in the subwavelength regime. In earlier work by

Sukenik *et al.* [12] on a similar system, the potential on atoms between conducting plates was investigated experimentally. In contrast to the evanescent parallel-plates guide suggested by Dowling and Gea-Banacloche [2], where the evanescent fields at a dielectric/vacuum interface arise due to the penetration of light through the interface into the vacuum region, the perfect conductor walls do not support evanescent modes but act to totally confine all fields introduced into the vacuum region. Because of its relative simplicity as a confining structure, the perfect conductor parallel-plate system has a distinguished history as a testing ground for the confinement effects in quantum electrodynamics [13]. Cavity quantum electrodynamics between dielectric surfaces have also been discussed [14] and the effects of atomic motion on the spontaneous emission within a Fabry-Pérot cavity has been examined [15]. However, as far as we know, the dynamics of atoms in such a fundamental system have not previously been investigated. It is the primary purpose of this paper to examine the essential ingredients of the theory leading to the description of atom dynamics between perfectly conducting parallel plates. Such a study should provide the initial steps towards a more comprehensive understanding of the nature of the forces in operation within atom guides in general.

Most of the atom guides that have been examined experimentally to date have relatively large dimensions, so that the guide operation has been multimode and consequently spontaneous emission has been effectively that in free space. Little work has been done on atom guides with subwavelength dimensions. As we emphasize later, in the subwavelength range the presence of a cutoff means that spontaneous emission can only be mediated by one or two possible modes and can be completely suppressed. The parallel-plate system, however, does not preclude a diffusive motion of atoms in directions parallel to the plates. The undesirable diffusive motion can be eliminated by closing the plates system so that it forms a cylindrical structure. Spontaneous emission in circular cylindrical structures has recently been considered by Rippin and Knight [16] and by Nha and Jhe [17]. Here we concentrate on the parallel-plate system and emphasize the

subwavelength cavity dimension in the parallel-plate context. Our aims are to describe the forces that act on the atom, the manner in which such forces change with the state of motion, and the role of the Casimir-Polder and van der Waals-type potentials between parallel plates with subwavelength separations.

In Sec. II we write down the Hamiltonian for an atom coupled to the quantized field between the plates. We outline how this leads to the position-dependent dipole decay rate and to the evaluation of the potential acting on the atom in the absence of an excited electromagnetic cavity mode. In Sec. III we evaluate the forces acting on the center-of-mass motion of the atom when a cavity mode is excited at a frequency appropriately detuned from the atomic transition frequency. We emphasize the importance of the dependence of the dipole potential (associated with the excited cavity mode) on the velocity of the atom parallel to the plates. For any given parallel velocity this dynamic dipole potential combines with the van der Waals-type potential to form the total potential that determines the transverse motion of the atom. The characteristics of the motion subject to this potential, together with the translational effects of the longitudinal dissipative force, are examined in some detail in Secs. IV and V for two cases of dipole orientations, namely, dipole parallel and dipole normal to the plates. Section VI discusses the dynamic potential and illustrates the changes of the system characteristics with the motion of the atom parallel to the plates. Section VII contains conclusions and further comments.

## II. ATOM PLUS FIELD SYSTEM

The system consists of an atom of total mass  $M$ , characterized by its electric dipole moment  $\boldsymbol{\mu}$  of oscillation frequency  $\omega_0$  interacting with the electromagnetic field. The effective Hamiltonian can be written as

$$H = \frac{P^2}{2M} + U(\mathbf{R}) + \hbar \omega_0 \pi^\dagger \pi - \boldsymbol{\mu} \cdot \mathbf{E}(\mathbf{R}) + H_f, \quad (1)$$

where  $\mathbf{P}$  and  $\mathbf{R}$  are the momentum and position vectors of the atomic center of mass, which is assumed to be subject to a general potential  $U(\mathbf{R})$ . In the two-level approximation of the internal motion of the atom, the operators  $\pi$  and  $\pi^\dagger$  are lowering and raising operators for internal atomic states  $|e\rangle$  and  $|g\rangle$  such that  $\boldsymbol{\mu} = \langle \boldsymbol{\mu} \rangle_{eg} (\pi + \pi^\dagger)$ ;  $\mathbf{E}$  is the electric field operator and  $H_f$  is the electromagnetic field Hamiltonian.

The quantized fields between perfectly conducting plates are well known [18] and can be written in terms of transverse electric ( $s$ -polarized) and transverse magnetic ( $p$ -polarized) modes satisfying the electromagnetic boundary conditions at the plates. We write for  $\mathbf{E}$

$$\mathbf{E}(\mathbf{r}, t) = \sum_{\eta=s,p} \sum_n \int d\mathbf{k}_\parallel \{ a_\eta(\mathbf{k}_\parallel, n) \mathcal{F}_\eta(\mathbf{k}_\parallel, n, \mathbf{r}, t) + \text{H.c.} \}, \quad (2)$$

where  $a_\eta(\mathbf{k}_\parallel, n)$  is the boson operator for the field mode characterized by the quantum number  $n$ , wave vector  $\mathbf{k}_\parallel$ , polarization  $\eta$ , and mode function  $\mathcal{F}_\eta(\mathbf{k}_\parallel, n, \mathbf{r}, t)$  satisfying electromagnetic boundary conditions at the conducting

plates. Assuming that the parallel plates are positioned at  $z = 0$  and  $L$  we have the mode functions

$$\mathcal{F}_s(\mathbf{k}_\parallel, n, \mathbf{r}, t) = C(k_\parallel, n) \hat{\mathbf{k}}_\parallel \times \hat{\mathbf{z}} \sin\left(\frac{n\pi z}{L}\right) e^{i\mathbf{k}_\parallel \cdot \mathbf{r}_\parallel - i\omega(k_\parallel, n)t} \quad (3)$$

and

$$\mathcal{F}_p(\mathbf{k}_\parallel, n, \mathbf{r}, t) = \frac{-icC(k_\parallel, n)}{\omega(k_\parallel, n)} \left[ i\hat{\mathbf{k}}_\parallel \left(\frac{n\pi}{L}\right) \sin\left(\frac{n\pi z}{L}\right) - \hat{\mathbf{z}} k_\parallel \cos\left(\frac{n\pi z}{L}\right) \right] e^{i\mathbf{k}_\parallel \cdot \mathbf{r}_\parallel - i\omega(k_\parallel, n)t}, \quad (4)$$

where carets denote unit vectors and we have written  $\mathbf{r} = (\mathbf{r}_\parallel, z)$ ;  $C(k_\parallel, n)$  is a normalization factor given by

$$C(k_\parallel, n) = \left[ \frac{\hbar \omega(k_\parallel, n)}{\epsilon_0 A L f_n} \right]^{1/2}, \quad (5)$$

with  $f_0 = 2$  and  $f_n = 1$  for  $n > 0$ .  $A$  is the (large) surface area of the plates. Throughout,  $\omega(k_\parallel, n)$  is the mode frequency such that

$$\omega^2(k_\parallel, n) = c^2 \left[ k_\parallel^2 + \frac{n^2 \pi^2}{L^2} \right]. \quad (6)$$

A plot of  $\omega$  versus  $k_\parallel$  gives rise to a series of branches, one for each  $n$ , and it is easy to see that the minima of these branches (occurring at  $k_\parallel = 0$ ) are separated by frequency  $\Delta\omega$  given by

$$\Delta\omega = \frac{c\pi}{L}. \quad (7)$$

The branch separation therefore increases with decreasing  $L$ . The large value of  $\Delta\omega$  will be emphasized as a special feature here for cavities with typically subwavelength dimensions.

In the absence of any external influence, the atom interacts with the vacuum fields that are now constrained by the plates, leading to two types of physical effect. First, the spontaneous dipole emission rate of the atom is modified to  $\Gamma(\mathbf{R})$  and, second, the atom experiences energy shifts to both levels. The shift in the excited-state energy amounts to a shift of the transition frequency  $\omega_0$  and this modifies the detuning. This shift, albeit position dependent, introduces small modifications to the large value of detuning parameter assumed in this paper. The ground-state shift, on the other hand, is equivalent to a potential  $U_g(\mathbf{R})$ , which is specified below.

The emission rate  $\Gamma$  can be calculated straightforwardly using the golden rule based on the formalism above. The results emerge in the following form. For a dipole oriented parallel to the plates the emission rate can be written as [13,18]

$$\Gamma_\parallel(Z) = \Gamma_0 \sum_{n=0}^{[2L/\lambda]} \frac{3\lambda}{4L} \left\{ 1 + \left( \frac{n\lambda}{2L} \right)^2 \right\} \sin^2\left(\frac{n\pi}{L} Z\right), \quad (8)$$

where  $\Gamma_0$  is the free-space dipole emission rate

$$\Gamma_0 = \frac{\omega_0^3 |\langle \boldsymbol{\mu} \rangle_{eg}|^2}{3 \pi \hbar \epsilon_0 c^3}. \quad (9)$$

$\lambda = 2\pi c/\omega_0$  is the wavelength of the dipole transition and  $[2L/\lambda]$  is the integer part of the bracketed quantity.

For a dipole oriented normal to the plates we have

$$\Gamma_{\perp}(Z) = \Gamma_0 \left[ \frac{3\lambda}{4L} + \sum_{n=1}^{[2L/\lambda]} \frac{3\lambda}{2L} \left\{ 1 - \left( \frac{n\lambda}{2L} \right)^2 \right\} \cos^2 \left( \frac{n\pi}{L} Z \right) \right]. \quad (10)$$

However, the potential  $U_g$  cannot be calculated on the basis of the two-level approximation implicit in the Hamiltonian in Eq. (1) and the theory should incorporate contributions from all transitions involving the entire energy spectrum of the atom. For a dipole oriented parallel to the plates the potential can be written as [18]

$$U_g(Z) = - \sum_j \frac{\pi |\langle \boldsymbol{\mu} \rangle_{jg}|^2}{6 \epsilon_0 L^3} \times \int_0^{\infty} dx \frac{x^2 \cosh \left( \pi x \left[ \frac{2Z}{L} - 1 \right] \right)}{\sinh(\pi x)} \tan^{-1} \left( \frac{x \lambda_{jg}}{2L} \right), \quad (11)$$

where  $\lambda_{jg}$  is the wavelength associated with the transition between the  $j$ th level and the ground state. This potential has been analysed carefully by Suenik *et al.* [12], who distinguished two regimes of variation. The first regime is such that  $L \gg \lambda/2\pi$ , where  $\lambda$  is the wavelength of the  $3^2s_{1/2} \leftrightarrow 3^2p_{3/2}$  transition in sodium. This corresponds to the Casimir-Polder regime in which  $U_g$  assumes the form

$$U_g(Z) = - \frac{\pi^3 \hbar c \alpha_s}{4 \pi \epsilon_0 L^4} \left\{ \frac{3 - 2 \cos^2 \left[ \frac{\pi}{L} (Z - L/2) \right]}{8 \cos^4 \left[ \frac{\pi}{L} (Z - L/2) \right]} \right\}, \quad (12)$$

where  $\alpha_s$  is the atomic polarizability. The second case corresponds to the quasistatic image regime (the van der Waals limit)  $L < \lambda/2\pi$ , where  $U_g$  is

$$U_g(Z) = - \frac{|\langle \boldsymbol{\mu} \rangle_{eg}|^2}{6 \pi \epsilon_0 L^3} \sum_{\text{odd } n} \left\{ \frac{1}{(n - 2Z/L)^3} + \frac{1}{(n + 2Z/L)^3} \right\}. \quad (13)$$

This form of potential has been confirmed experimentally by Sandoghdar *et al.* [19] for the case of a micrometer-sized cavity. Since our main concern here will be with the small  $L$  (van der Waals) regime, specifically in the subwavelength range, we adopt the form given in Eq. (13) in our illustrations of the theory and comment briefly on the modifications that are likely to arise in the large- $L$  (Casimir-Polder) regime.

### III. DYNAMICS

The state of the motion of the atom between the plates can be altered by the excitation of one or more cavity modes. With one of the modes excited with sufficient intensity, the atom experiences radiation forces of the type familiar in the case of atoms subject to spatially varying light in free space [20,21]. In general, the average radiation forces emerge in the adiabatic approximation using the optical Bloch equations for the internal atomic density matrix elements in which the position and momentum of the center of mass are replaced by their expectation values. The validity of this semi-classical approximation requires that the spatial extent of the atomic wave packet be much smaller than the wavelength of the radiation field. This is assumed to hold in this paper. The solution of the optical Bloch equations shows that the dipole moment and hence the forces acting on the atom relax to steady-state values within a time of the order  $\Gamma^{-1}$  from the instant at which the light field is switched on. Since this time is typically much shorter than observation times involved in the channeling of atoms through the structure, we need only concentrate on the steady state forces.

In the steady state, the atom is subject to a dissipative force  $\langle \mathbf{F}_{\xi} \rangle$ , which can be written as [22]

$$\langle \mathbf{F}_{\xi}(k_{\parallel}, n, Z) \rangle = 2 \hbar \Gamma_{\xi}(Z) \Omega_{\xi}^2(k_{\parallel}, n, Z) \times \left\{ \frac{\nabla \Theta}{\Delta^2(k_{\parallel}, n, \mathbf{V}) + 2 \Omega_{\xi}^2(k_{\parallel}, n, Z) + \Gamma_{\xi}^2(Z)} \right\}, \quad (14)$$

where  $\xi$  is either  $\parallel$  or  $\perp$ , depending on the dipole orientation, and  $\Theta$  is the mode phase. In view of Eqs. (3) and (4) we have for all modes

$$\nabla \Theta = \mathbf{k}_{\parallel}. \quad (15)$$

This immediately fixes the direction of the dissipative force as parallel to the plates in the direction of mode propagation.  $\Delta(k_{\parallel}, n, \mathbf{V})$  is the dynamic detuning, defined by

$$\Delta(k_{\parallel}, n, \mathbf{V}) = \omega(k_{\parallel}, n) - \omega_0 - \nabla \Theta \cdot \mathbf{V} = \Delta_0 - k_{\parallel} V_{\parallel}. \quad (16)$$

$\Omega_{\xi}(k_{\parallel}, n, Z)$  is a position-dependent Rabi frequency associated with the cavity mode of type  $\eta$  and is defined by

$$\hbar \Omega_{\xi}(k_{\parallel}, n, Z) = |\langle \boldsymbol{\mu} \rangle_{eg} \cdot \mathcal{F}_{\eta}(k_{\parallel}, n, Z)|_{\xi}, \quad (17)$$

where  $\mathcal{F}_{\eta}$  is either  $s$  polarized or  $p$  polarized, as given in Eqs. (3) and (4).

In the presence of a cavity mode the atom also becomes subject to a light-induced force derivable from the dipole potential associated with the cavity mode. This too depends on the dipole orientation as well as the type of cavity mode and can be written as [23]

$$U_{\xi}(k_{\parallel}, n, Z) = \frac{\hbar \Delta(k_{\parallel}, n, \mathbf{V})}{2} \ln \left[ 1 + \frac{2 \Omega_{\xi}^2(k_{\parallel}, n, Z)}{[\Delta^2(k_{\parallel}, n, \mathbf{V}) + \Gamma_{\xi}^2(Z)]} \right]. \quad (18)$$

The classical motion of the center of mass of the atom is determined by the solution of the equation of motion

$$M \left( \frac{d^2 \mathbf{R}}{dt^2} \right)_\xi = \langle \mathbf{F}_\xi \rangle - \nabla U_{T\xi}(Z), \quad (19)$$

with  $U_{T\xi}(Z)$  the total potential

$$U_{T\xi}(Z) = U_\xi(Z) + U_g(Z), \quad (20)$$

where  $U_\xi(Z)$  and  $U_g(Z)$  are given by Eqs. (18) and (13). Strictly speaking, the atom ‘‘feels’’ different van der Waals potentials associated with the ground state and the excited state. We have appealed to the semiclassical approximation on including in Eq. (20) the ground-state van der Waals potential  $U_g$  in the total potential. This is consistent with the approximations discussed above where the position and momentum of the center of mass are replaced by their expectation values.

Since  $\langle \mathbf{F}_\xi \rangle$  always points in a direction parallel to the plates, the equation of motion decouples naturally into two separate equations, corresponding to the parallel and normal components of the atom position vector  $\mathbf{R} = (\mathbf{r}_\parallel, Z)$ . We have

$$M \left( \frac{d^2 \mathbf{r}_\parallel}{dt^2} \right)_\xi = \langle \mathbf{F}_\xi \rangle, \quad (21)$$

$$M \left( \frac{d^2 Z}{dt^2} \right)_\xi = - \frac{dU_{T\xi}}{dZ}. \quad (22)$$

Note, however, that  $V_\parallel$ , the magnitude of the velocity in the parallel direction, appears in the second equation of motion due to the explicit dependence of  $U_\xi(Z)$  on  $\Delta(k_\parallel, n, \mathbf{V})$ .

#### IV. PARALLEL MOTION

The solution of Eq. (21) can be obtained analytically once we observe that we can write

$$M \frac{dV}{dt} = 2\hbar\Gamma\Omega^2 \left\{ \frac{k}{(\Delta_0 - kV)^2 + 2\Omega^2 + \Gamma^2} \right\}, \quad (23)$$

where we have dropped the  $\xi$  label of the mode. Without loss of generality, we have assumed propagation along the  $x$  axis and set  $V_x = V$ . If the mode is excited at  $t=0$  when the atom is stationary [ $V(t=0)=0$ ] at the space point  $(\mathbf{0}, Z)$ , Eq. (23) can be integrated straightforwardly. At time  $t>0$  the longitudinal velocity emerges from the solution of the equation

$$a_1 V^3 + a_2 V^2 + a_3 V = t, \quad (24)$$

where the  $a$  coefficients are given by

$$a_1 = - \frac{a_2 k}{3\Delta_0} = \frac{k^2 \Gamma_0 M}{3F_0 \Omega^2 \Gamma}, \quad (25)$$

$$a_3 = \frac{\Gamma_0 M (\Delta_0^2 + 2\Omega^2 + \Gamma^2)}{\Gamma F_0 \Omega^2},$$

with  $F_0 = 2\hbar k \Gamma_0$ , a convenient scaling force for this system.

The distance traveled by the atom after time  $t$  has elapsed is obtained by integrating the velocity  $V(t)$ . We have formally

$$x(t) = \int_0^t V(t) dt. \quad (26)$$

With the help of Eq. (24), Eq. (26) yields straightforwardly

$$x(t) = \frac{3}{4} a_1 V^4 + \frac{2}{3} a_2 V^3 + \frac{1}{2} a_3 V^2. \quad (27)$$

The parameters needed for the evaluation of the velocity and the distance traveled are in fact fixed by the requirement of trapping, as we explain in Sec. V.

## V. TRANSVERSE TRAPPING

### A. Typical parameters

For a negatively detuned atom and for low velocities, Eq. (18) should provide a quasi-harmonic potential that confines the atoms in the region of the minimum of  $U_{T\xi}$ . In order to see this, it is instructive to focus on a typical physical situation.

We therefore consider the  $3^2s_{1/2} \leftrightarrow 3^2p_{3/2}$  transition in sodium ( $\lambda = 589$  nm) and assume that the cavity mode is excited by a laser of intensity comparable to that adopted by Renn *et al.* [4] in their experiment. We define a free-space Rabi frequency  $\Omega_0$  by

$$\Omega_0^2 = \frac{|\langle \boldsymbol{\mu} \rangle_{eg}|^2 I}{2\hbar^2 \epsilon_0 c}, \quad (28)$$

with  $I \approx 10^7$  W m<sup>-2</sup> the intensity of the laser used to excite this mode and  $|\langle \boldsymbol{\mu} \rangle_{eg}| \approx 2.6 e a_B$ , where  $a_B$  is the Bohr radius. This dipole matrix element is consistent with the free-space lifetime of 16.3 ns [24]. With  $I \approx 10^7$  W m<sup>-2</sup> the free-space Rabi frequency is obtained as  $\Omega_0 = 8.56 \times 10^9$  s<sup>-1</sup>.

For the plate separation we assume the subwavelength value adopted by Sandoghdar *et al.* [11]

$$L = 500 \text{ nm} \approx 0.85\lambda. \quad (29)$$

There are two immediate consequences of this subwavelength plate separation. First, the branch frequency separation, defined in Eq. (7), is very large:  $\Delta\omega = c\pi/L = 1.89 \times 10^{15}$  s<sup>-1</sup>. This is of the same order of magnitude as  $\omega_0$ . Second, the sum over  $n$  in Eqs. (8) and (10) terminates at  $n=1$ . The first manifestation of small  $L$  permits large detuning and so facilitates single-mode performance; the second indicates that spontaneous emission is effected by a single branch for the parallel dipole orientation. For the normal dipole orientation spontaneous emission receives an additional contribution from the fundamental mode. We may therefore assume a large value for the detuning  $\Delta_0 = \omega - \omega_0$ . We consider first negative  $\Delta_0$  and write

$$\Delta_0 = -6.0 \times 10^2 \Gamma_0, \quad (30)$$

where  $\Gamma_0$  is given by Eq. (9), yielding  $\Gamma_0 \approx 6.13 \times 10^7$  s<sup>-1</sup>. This corresponds to  $|\Delta_0| = 36.78$  GHz.

Finally, it is convenient to define two scaling parameters: a scaling force  $F_0$  and a scaling potential energy  $U_0$ . With  $\Delta_0$  defined in Eq. (30) and with  $\omega_0$  corresponding to  $\lambda = 589$  nm, it is straightforward to deduce the magnitude of the parallel wave vector  $k_\parallel$  using Eq. (6). The scaling parameter  $F_0$  depends on  $k_\parallel$  and is defined by

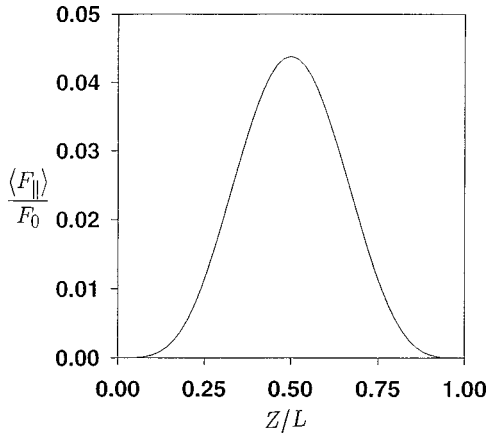


FIG. 1. Variation across the plates of the quasistatic dissipative force acting on a sodium atom when the  $n=1$   $p$ -polarized cavity mode is excited. Here the electric dipole matrix element is oriented *parallel* to the plates; see the text in Sec. V A for the parameters used.

$$F_0 = 2\hbar k_{\parallel} \Gamma_0 \approx 1.38 \times 10^{-19} \text{ N}, \quad (31)$$

while for the scaling potential energy  $U_0$  we write

$$U_0 = \frac{1}{2} \hbar \Gamma_0 = 3.23 \times 10^{-27} \text{ J}. \quad (32)$$

This value of  $U_0$  is equivalent to about 4.9 MHz. In the figures below, force is measured in units of  $F_0$  and potential energy in units of  $U_0$ .

### B. Dipole parallel to the plates

With the dipole oriented parallel to the plates and with the  $n=1$   $p$ -polarized mode excited we have a position-dependent Rabi frequency given by

$$\Omega_{p\parallel}(Z) = \sqrt{2} \Omega_0 \left( \frac{\lambda}{2L} \right) \sin \left( \frac{\pi Z}{L} \right). \quad (33)$$

The quasistatic dissipative force on the atom is given by Eq. (14). With the dipole oriented parallel to the plates and in a situation corresponding to the above choice of parameters a dissipative force field is set up with variation across the plates as shown in Fig. 1. It can be seen from this figure that atoms located at the center of the guide receive the strongest force parallel to the plates. The corresponding potential profiles are depicted in Figs. 2(a) and 2(b). It can be deduced

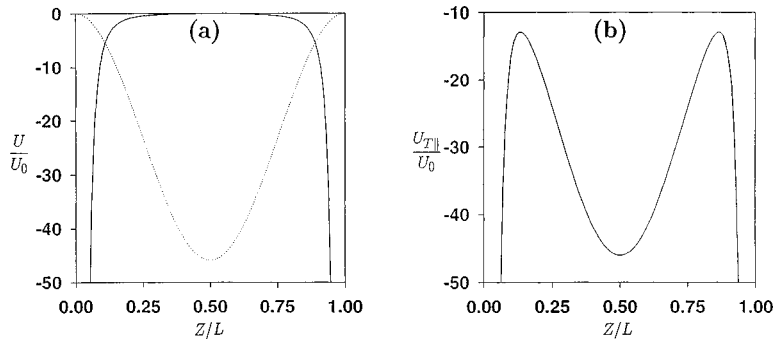


FIG. 2. Potentials of the sodium atom between the plates under the conditions of Fig. 1 when the dipole is *parallel* to the plates: (a) the dipole potential (dotted curve) and the van der Waals potential (full curve) and (b) the total potential.

from these figures that, from a quantum-mechanical point of view, the ground state of the transverse motion will correspond to a solution of the one-dimensional Schrödinger equation with only the van der Waals potential and so the vibrational ground-state distribution should peak near the plates. Atoms in their ground vibrational state are thus localized in the potential well near the plates. However, a solution of the one-dimensional Schrödinger equation with  $U_{T\parallel}(z)$  as the potential must also exist for which the atomic wave function peaks in the vicinity of the central minimum associated with the dipole potential shown in Fig. 2. This is an excited state of the vibrational motion. It can be seen from Fig. 2 that for the parameters assumed above, the central well depth is approximately  $45U_0 \approx 220.5$  MHz. This is sufficiently deep to allow several quasiharmonic trapping (vibrational) states. The vibrational frequency  $\delta\omega_1$  can be estimated simply using the parabolic approximation

$$\delta\omega_1 = \left\{ \frac{2}{M} \frac{d^2 U_{\parallel}}{dZ^2} \right\}_{Z=L/2}^{1/2}. \quad (34)$$

We have explicitly

$$\delta\omega_1 = \left( \frac{4\hbar \pi^2 \Omega^2 \Delta}{(\Delta^2 + 2\Omega^2) L^2 M} \right)^{1/2}_{Z=L/2}. \quad (35)$$

It is not difficult to check that with the above parameter values for sodium in the  $n=1$   $p$ -polarized mode within the parallel plate system described above we have

$$\delta\omega_1 \approx 1.96 \times 10^7 \text{ s}^{-1}. \quad (36)$$

The precise details of the vibrational energy levels can be obtained straightforwardly by the numerical solution of the one-dimensional Schrödinger equation involving the full  $U_{T\parallel}(Z, V)$  potential.

### C. Dipole normal to the plates

With the dipole oriented normal to the plates and the  $n=1$   $p$ -polarized cavity mode excited, the Rabi frequency is

$$\Omega_{p\perp} = \sqrt{2} \Omega_0 \left( 1 - \frac{\lambda^2}{4L^2} \right)^{1/2} \cos \left( \frac{\pi Z}{L} \right). \quad (37)$$

The quasistatic dissipative force corresponding to the same choice of parameters as in Sec. V A is shown in Fig. 3 and

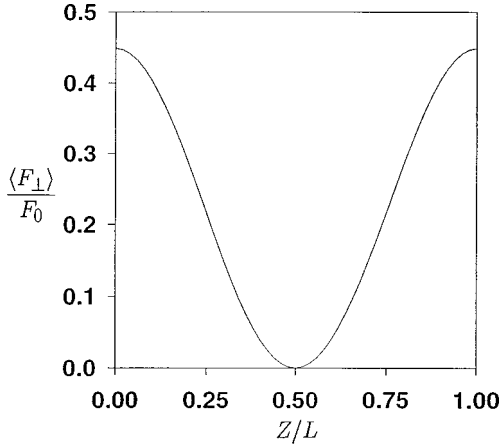


FIG. 3. Variation across the plates of the quasistatic dissipative force acting on a sodium atom when the  $n=1$   $p$ -polarized cavity mode is excited. Here the electric dipole matrix element is oriented *normal* to the plates; see the text in Sec. V A for the parameters used.

the corresponding potential profile  $U_{T\perp}(Z)$  is depicted in Fig. 4. In contrast to the case of parallel dipole orientation, the negative detuning dipole potential has no minimum at the center of the guide. It in fact enhances the effects of the van der Waals potential, which tends to attract the atoms towards the plates. Clearly, the solutions of the Schrödinger equation with  $U_{T\perp}(Z)$  as the potential will always have the atomic vibrational ground-state distribution peaking in the vicinity of the plates. A reversal of the sign of detuning, however, leads to a dipole potential of the opposite sign to that shown in Fig. 4(a). On adding the van der Waals potential to this we have Fig. 4(c). It is easy to see that transverse trapping of atoms in the central region is possible for this case too. However, in this situation the central region for dipoles normal to the interface is a dark region, so the atoms are subject to a minimum of the dissipative force and channeling can only occur for atoms with an initial longitudinal velocity. This case of a subwavelength structure should be contrasted with the case of structures of much larger dimensions where the emission rate is practically equal to  $\Gamma_0$  in the central region of the structure.

## VI. DYNAMIC POTENTIAL

The main desirable feature of atom dynamics in this context relies on the ability to confine the atoms within the cen-

tral region of the structure while being driven in the parallel direction by the dissipative force. It therefore depends on the depth of the central well associated with the dipole potential. In the preceding section we have explored the low-velocity properties of this potential and it is important now to examine how this varies with changing velocity.

In Figs. 5(a) and 5(b) we display the variation of the parallel potential  $U_{T\parallel}(L/2, t)$  with time, which is measured from the instant the mode is excited. It can be seen that the depth of the well decreases with time as the velocity increases, reaching a small depth at large  $t$  when the dipole well becomes too shallow to trap the atoms. They are then susceptible to falling in the ever-present deep well near the plates due to the van der Waals-type potential. Figures 6(a) and 6(b) display the changes in the dipole potentials with velocity for negative and positive detuning, respectively, both when the dipole orientation is normal to the plates. It can be seen that in Fig. 6(a) the potential increasingly become shallower with increasing velocity, with the relevant variations occurring closer and closer to the plates, while in Fig. 6(b) the central potential well becomes deeper with increasing velocity.

Figure 7 displays the evolution of the longitudinal dissipative force acting on the atom and the corresponding velocity when the dipole is parallel to the plates and negative detuning. It can be seen that the longitudinal dissipative force asymptotically approaches vanishing values while the velocity tends to a constant value.

## VII. COMMENTS AND CONCLUSIONS

From the cases illustrated above, it is clear that the relevant characteristics of the system depend not only on the magnitude and sign of the parameters but also on the dipole orientation. In order to maintain the central transverse trapping while heating initially slow atoms with negative detuning and parallel dipole orientation between the plates, appropriate parameters should be chosen in order to maintain a sufficient central well depth with increasing parallel velocity. For initially energetic atoms channeling can be achieved by an opposing force due to a mode propagating in an opposite direction to the atomic velocity, in which case the atoms experience an increasingly deeper central well as their velocity decreases. For the same parameters, we have seen that the same mode does not give rise to a central potential well for dipoles normal to the plates and the atoms tend to be at-

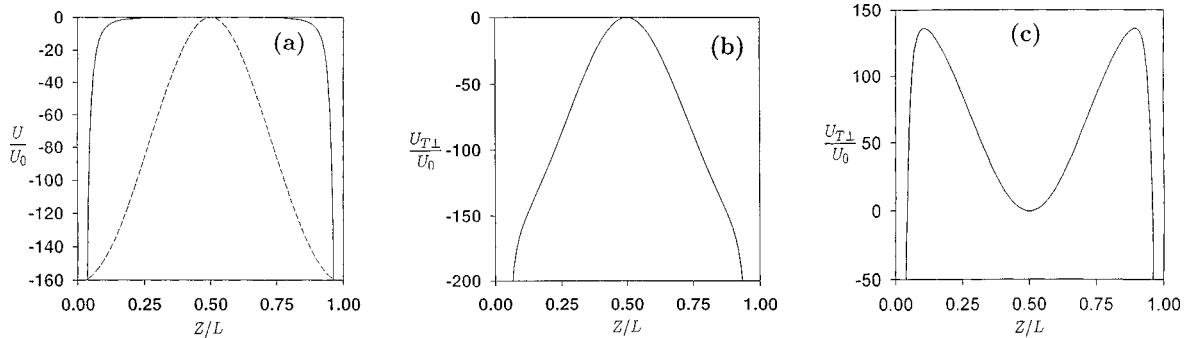


FIG. 4. Potential of the sodium atom between the plates for the case of dipole *normal* to the plates: (a) the dipole potential with negative detuning (dotted curve) and the van der Waals potential (full curve), (b) the total potential for the negative detuning case, and (c) the total potential for the positive detuning case.

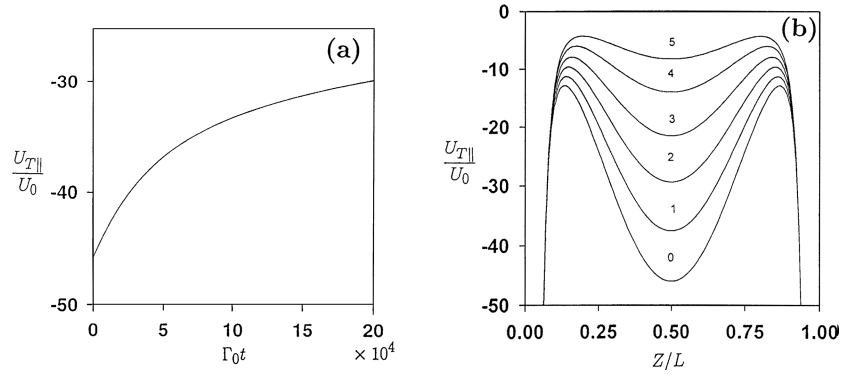


FIG. 5. Dipole *parallel* to the plates. (a) Dynamic dipole potential at the center of the guide as a function of time and (b) variation of the potential across the plates for different values of the parallel velocity. The labels 0–5 stand for  $V=0.0, 0.1, 0.25, 0.5, 1.0,$  and  $2.0 \times 10^4 \text{ ms}^{-1}$ .

tracted to the plates. Once the atoms are in the vicinity of the walls, they may then interact strongly with the wall, become adsorbed to it, or be ejected with a thermal velocity.

In the parallel dipole orientation with negative detuning, the van der Waals potential becomes the dominant trapping potential when the velocity of the atom is too high and the dipole potential is too shallow to trap the atom. The atom then tends to be localized near the walls.

For dipoles normal to the plates and positive detuning the atoms can be confined within the central (dark) region, experiencing a minimum longitudinal force. They would then tend to drift in a plane parallel to the plates while confined in a vibrational state. The atoms encounter an increasingly deeper potential well as their velocity increases.

In the case of plate separations  $L \gg \lambda/2\pi$ , the Casimir-Polder force given by Eq. (12) replaces the van der Waals potential. Sukenik *et al.* [12] have shown that, despite the differences between the potentials in these two regimes, the relevant variations of potential in the vicinity of the plates are quite similar. We therefore expect a similar behavior in the Casimir-Polder limit as regards trapping between parallel plates. The main feature distinguishing the two regimes is that for large  $L$  the structure is multimode in principle and in the axial region spontaneous emission is practically that in free space. In contrast, the small- $L$  regime offers single-mode operation in addition to the inherent limitations in the number of modes that can contribute to spontaneous emission at subwavelength separations.

It is important to note that the atoms confined transversely in the parallel-plate system are prone to a diffusive increase of the atomic momentum parallel to the plates. Translated into spatial coherence, this means that a single spontaneous emission event reduces the atomic longitudinal coherence length to a wavelength, in a fashion similar to the situation arising in the experiment by Pfau *et al.* [25], who studied coherence in the diffraction of atoms by a standing light wave. This is the main reason why a parallel-plate system cannot in general be employed as an efficient atom guide.

The fact that the transverse atomic motion is describable in terms of vibrational states and that the spontaneous emission is modified due to the discrete mode structure between the plates suggest that atomic coherence may be preserved along this direction. This issue may be investigated along the lines of Castin and Dalibard [26], who considered Sisyphus cooling in one-dimensional optical molasses and took account of the vibrational states of the atom in the potential associated with the standing wave. Theoretical work on Sisyphus cooling in the context of evanescent fields has been done by Nha and Jhe [27].

In this paper we have separated the cases of parallel and transverse dipole orientations. However, for slow atoms the orientation of the dipole moment is determined by the polarization of the driving field. For motion perpendicular to the walls different orientations of the dipole moment can be nonadiabatically coupled due to changing mode polarisation. This problem will not be pursued any further here.

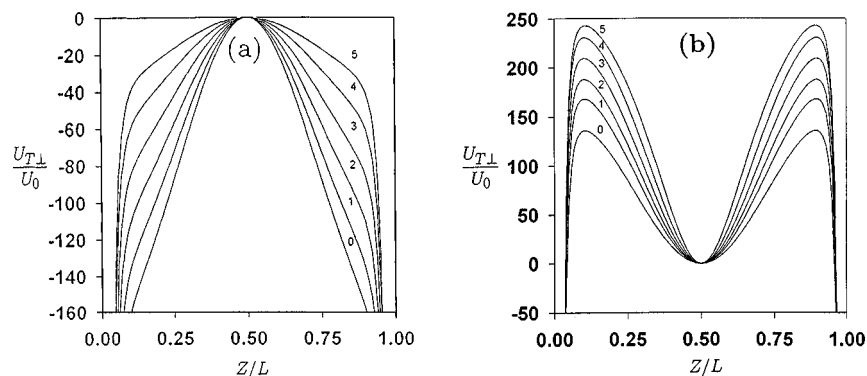


FIG. 6. Dipole *normal* to the plates. Variation of the potential across the plates for different values of the parallel velocity: (a) negative detuning and (b) positive detuning. The labels 0–5 stand for  $V=0.0, 0.1, 0.25, 0.5, 1.0,$  and  $2.0 \times 10^4 \text{ ms}^{-1}$ .

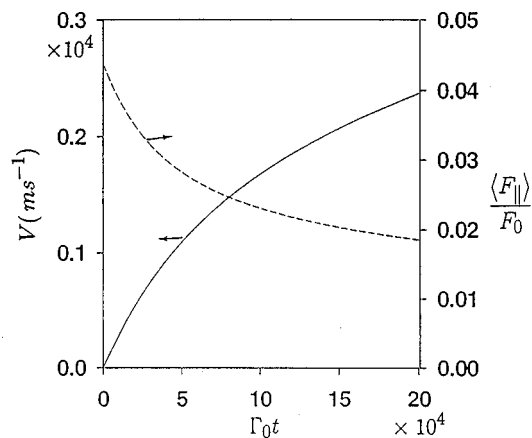


FIG. 7. Dipole *parallel* to the plates with negative detuning: evolution with time of the parallel velocity (full curve) and the dissipative force acting on the atom (dashed curve).

Besides exploring the nature of the dynamics for atoms within subwavelength structures, this paper has shed light on the role of the van der Waals potential in the same context. We have shown that the effects of the van der Waals forces

are restricted to a relatively narrow region near the walls and that the main trapping features are determined by the driving fields. This conclusion has been reached only following the evaluations illustrated here where use of typical parameters has allowed the dipole potential and the van der Waals potential to be compared and their regions of variations established.

The general features explored here for the case of the parallel-plate system are relevant for the case of atoms moving within cylindrical structures. In fact, the above considerations of the parallel-plate system have now paved the way for considering subwavelength cylindrical structures that could be used as efficient atom guides. Work along these lines is now in progress and the results will be reported in due course.

#### ACKNOWLEDGMENTS

We are grateful to E. A. Hinds and M. G. Boshier for useful discussions, and to M. Bowa'aneh for his help with the computational aspects of this work. S. Al-Awfi wishes to acknowledge financial support from the Saudi Arabian government.

- 
- [1] C. S. Adams and E. Riis, *Prog. Quantum Electron.* **21**, 1 (1997).
- [2] J. P. Dowling and J. Gea-Banacloche, *Adv. At., Mol., Opt. Phys.* **37**, 1 (1996).
- [3] M. Schiffer, G. Wokurka, M. Rauner, S. Kuppens, K. Sengstock, and W. Ertmer (unpublished).
- [4] M. J. Renn, D. Montgomery, O. Vdovin, D. Z. Anderson, C. E. Wieman, and E. A. Cornell, *Phys. Rev. Lett.* **75**, 3253 (1995).
- [5] M. A. Ol'Shanii, Y. B. Ovchinnikov, and V. S. Letokhov, *Opt. Commun.* **98**, 77 (1993).
- [6] S. Marksteiner, C. M. Savage, P. Zoller, and S. L. Rolston, *Phys. Rev. A* **50**, 2680 (1994); C. M. Savage, D. Gordon, and T. C. Ralph, *ibid.* **52**, 4741 (1995).
- [7] W. Jhe, M. Ohtsu, H. Hori, and S. R. Freiberg, *Jpn. J. Appl. Phys., Part 2* **33**, L1680 (1994).
- [8] H. Ito, K. Sakaki, T. Nakata, W. Jhe, and M. Ohtsu, *Opt. Commun.* **115**, 57 (1995).
- [9] M. J. Renn, E. A. Donley, E. A. Cornell, C. E. Wieman, and D. Anderson, *Phys. Rev. A* **53**, R648 (1996).
- [10] H. Ito, K. Sakaki, M. Ohtsu, and W. Jhe, *Appl. Phys. Lett.* **70**, 2496 (1997).
- [11] V. Sandoghdar, C. I. Sukenik, S. Haroche, and E. A. Hinds, *Phys. Rev. A* **53**, 1919 (1996).
- [12] C. I. Sukenik, M. G. Boshier, D. Cho, V. Sandoghdar, and E. A. Hinds, *Phys. Rev. Lett.* **70**, 560 (1993).
- [13] E. A. Hinds, *Adv. At., Mol., Opt. Phys.* **28**, 237 (1991); **2**, 1 (1993).
- [14] H. Nha and W. Jhe, *Phys. Rev. A* **54**, 3505 (1996).
- [15] M. Wilkens, Z. Bialyncka-Birula, and P. Mystre, *Phys. Rev. A* **45**, 477 (1992).
- [16] M. A. Rippin and P. L. Knight, *J. Mod. Opt.* **47**, 807 (1996).
- [17] H. Nha and W. Jhe, *Phys. Rev. A* **56**, 2213 (1997).
- [18] G. Barton, *Proc. R. Soc. London, Ser. A* **320**, 251 (1970); **410**, 141 (1987); **410**, 175 (1987); **453**, 2461 (1997).
- [19] V. Sandoghdar, C. I. Sukenik, E. A. Hinds, and S. Haroche, *Phys. Rev. Lett.* **68**, 3432 (1992).
- [20] J. P. Gordon and A. Ashkin, *Phys. Rev. A* **21**, 1606 (1980).
- [21] J. Dalibard and C. Cohen-Tannoudji, *J. Opt. Soc. Am. B* **2**, 1707 (1985).
- [22] M. Babiker, W. L. Power, and L. Allen, *Phys. Rev. Lett.* **73**, 1239 (1994).
- [23] L. Allen, M. Babiker, V. E. Lembessis, and W. K. Lai, *Phys. Rev. A* **54**, 4259 (1996).
- [24] M. Wilkens, *Phys. Rev. A* **47**, 2366 (1993).
- [25] T. Pfau, S. Spälter, C. Kurtsiefer, C. Ekstrom, and J. Mlynek, *Phys. Rev. Lett.* **73**, 1223 (1994).
- [26] Y. Castin and J. Dalibard, *Europhys. Lett.* **14**, 761 (1991).
- [27] H. Nha and W. Jhe, *Phys. Rev. A* **56**, 729 (1997).